AIP | Applied Physics Letters

Formation of nickel germanide contacts to Ge nanowires

N. S. Dellas, S. Minassian, J. M. Redwing, and S. E. Mohney

Citation: Appl. Phys. Lett. **97**, 263116 (2010); doi: 10.1063/1.3533808
View online: http://dx.doi.org/10.1063/1.3533808
View Table of Contents: http://apl.aip.org/resource/1/APPLAB/v97/i26
Published by the AIP Publishing LLC.

Formation of nickel germanide contacts to Ge nanowires

N. S. Dellas,[1] S. Minassian,[2] J. M. Redwing,[1,3] and S. E. Mohney[1,3,a)]
[1]*Department of Materials Science and Engineering, The Pennsylvania State University, University Park, Pennsylvania 16802, USA*
[2]*Department of Chemical Engineering, The Pennsylvania State University, University Park, Pennsylvania 16802, USA*
[3]*Materials Research Institute, The Pennsylvania State University, University Park, Pennsylvania 16802, USA*

(Received 14 November 2010; accepted 14 December 2010; published online 30 December 2010)

Nickel germanide contacts are expected to play an important role in Ge-based electronics similar to that of their nickel silicide counterparts in Si devices. Here we have studied the solid state reaction between Ni contact pads and Ge nanowires. We observe the formation of axial nickel germanide segments after annealing at temperatures as low as 300 °C for 2 min. The nickel germanide segments are polycrystalline, without an epitaxial relationship to the Ge nanowire, in contrast to observations of epitaxial nickel silicide formation from Si nanowires. The crystal structure of the nickel germanide phase is consistent with the Ni_2In prototype structure. Annealing above 400 °C results in fracture in the nickel germanide segment; however, nickel germanide segments as long as 1.7 μm can be formed by annealing at 400 °C for 5 min. © *2010 American Institute of Physics*. [doi:10.1063/1.3533808]

Germanium nanowires (GeNWs) have attracted considerable interest for applications such as field-effect transistors[1] and chemical and biological sensors.[2] Germanium NWs in particular are interesting because of the higher carrier mobilities of Ge compared to Si.[3] Furthermore, Ge has a larger exciton Bohr radius than Si,[4] making quantum confinement effects more readily observable in larger-diameter GeNWs. However, electrical contacts may limit the performance of semiconductor nanowire devices because of the nature of the Schottky barrier present at the metal/semiconductor interface.

Silicides—intermetallic phases that often form through the solid state reaction of Si and a metal layer—are quite commonly used as contacts in Si-based technology because of their compatibility with the self-aligned silicide (salicide) process. In Si-based technology, NiSi is a common Ohmic contact because of its low electrical resistivity, reasonable thermal stability, and ability to form in small dimensions.[5] In the binary Ni-Si system, a number of intermetallic phases can and do form in thin-film contacts, and great attention has been paid to the phase formation sequence when Ni films react with Si wafers.

For Ge-based electronics, it is reasonable to expect that a process analogous to the Ni-salicide process for germanide formation would be useful for contacts to Ge-based devices.[6] Due to the relative immaturity of Ge-based technology, considerably less work has been completed to understand the phase formation sequence and thermal stability of phases in the Ni-Ge system compared to those in the Ni-Si system. For the reaction of Ni thin films on Ge wafers, the observed phase formation sequence begins with the formation of a Ni-rich germanide [orthorhombic Ni_2Ge,[7] hexagonal Ni_2Ge,[8] monoclinic Ni_5Ge_3,[9] or hexagonal Ni_3Ge_2 (Ref. 10)], and researchers have reported the formation of the different phases listed above under similar annealing conditions. Next, NiGe forms[11] and remains thermally stable up to temperatures in excess of 500 °C when agglomeration of the film begins. The Ni-rich germanides are not reported to form with an epitaxial relation to the Ge substrate, but NiGe has been reported to form epitaxially.[12]

Previous researchers have studied the reaction of Ni and SiNWs.[13–15] In contrast to the reaction of Ni films on Si wafers, sequential phase formation is not reported in Ni/SiNW reactions, and the formation of metastable phases not commonly seen in thin-film reactions has been observed.[15] Different silicides form depending on the SiNW growth direction and other factors, but many of these phases grow with an epitaxial relation to the SiNW.[13–15] Solid state reactions of Ni films with GeNWs may also differ from their thin-film counterparts, and limited work has been performed on germanide formation in any metal-GeNW system, with the notable exception of Cu_3Ge contacts to GeNWs.[16]

In this paper, GeNWs were grown by the vapor-liquid-solid method from 3 nm thick Au films on oxidized Si wafers. GeH_4 was used as the precursor gas for the GeNW growth. The growth temperature was 300 °C, the reactor pressure was 50 Torr, and the growth time was 80 min. GeNWs were then sonicated from the growth substrate into isopropanol, and electron-transparent contacts were fabricated by a method described in detail elsewhere.[15] In the present work, a deionized water soak for 90 s was used to remove the native oxide on the GeNWs prior to e-beam evaporation of 80 nm thick Ni contacts, which differs from the use of buffered hydrofluoric acid to remove the native oxide on SiNWs. Samples were then annealed *ex situ* in a rapid annealing furnace (AG Associated Heat Pulse 610) in ultrahigh purity Ar at temperatures of 300, 350, 400, 450, 500, and 600 °C for 2 min each. Transmission electron microscopy (TEM) was performed using a JEOL EM-2010F field-emission TEM with a Gatan double-tilt holder.

Axial nickel germanide segments begin to form after 2 min at 300 °C, as shown in Fig. 1(a). The average length of the nickel germanide segment after 2 min at 300 °C is 20

a)Electronic mail: mohney@ems.psu.edu.

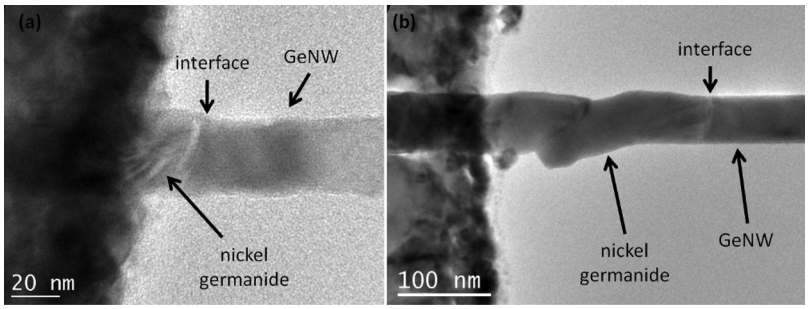

FIG. 1. (a) TEM image of a Ni contact pad on a GeNW annealed at 300 °C for 2 min and (b) TEM image of a sample annealed at 350 °C for 2 min. The darker contrast in the GeNW near the nickel germanide/GeNW interface is caused by strain.

nm. After annealing at 350 °C for 2 min, the nickel germanide segment is observed to increase in length to 230 nm on average [Fig. 1(b)]. The axial nickel germanide segment is polycrystalline with grain boundaries that extend across the entire cross-section of the NW. Selected area electron diffraction (SAED) patterns (Fig. 2) taken from individual grains of nickel germanide were matched to the Ni_2In prototype structure with the space group $P6_3/mmc$.[17] We measured lattice parameters of $a=3.95$ Å and $c=5.18$ Å, which is in relatively good agreement with values determined by x-ray diffraction ($a=3.947$ Å and $c=5.037$ Å) for different phases of nickel germanide in the Ni_2In prototype structure. Interestingly, we find that nickel germanide grains are misaligned from each other by only 2°–3°. The low angle of the grain boundaries, suggestive of low-energy interfaces, may explain why different grains are able to form during the growth of the nickel germanide segment. Furthermore, we find that the growth direction of the GeNW does not affect the phase formation. For GeNWs with [111], [112], and [110] growth directions the same nickel germanide phase is observed, unlike the SiNW growth direction dependence of solid-state reactions between Ni and SiNWs.[15]

The match of the SAED patterns from the TEM to the prototype structure Ni_2In suggests that the stoichiometry of the nickel germanide phase is Ni_2Ge; however, there are a number of different phases reported with very similar crystal structures, including Ni_2Ge, Ni_5Ge_3, $Ni_{19}Ge_{12}$, $Ni_{17}Ge_{12}$, and Ni_3Ge_2.[17] The Ni_2In structure is similar to the NiAs prototype structure with the exception that there is an additional Ni sublattice present in the Ni_2In structure. The difference between the Ni_xGe stoichiometries listed above is due to vacancies on one of the Ni sublattices, causing deviation from the ideal Ni:(Ge or In) stoichiometry of 2:1. According to Ellner *et al.*,[18] vacancies on one of the Ni sublattices result in different stoichiometries in the B8 phase region of the Ni-Ge system. Work performed by Larsson and Withers[19] using electron diffraction suggested that these vacancies may be ordered in many of the phases, giving rise to the different stoichiometries of the related nickel germanides; however, we have not been able to identify any ordering, as might be revealed by electron diffraction spots in addition to those expected from the Ni_2In prototype structure. We do not rule out the possibility that vacancies are present; however, based on the work of Larsson and Withers, the phase that seems most consistent with diffraction data obtained herein is Ni_3Ge_2. Larsson and Withers reported that this phase was the only one within the B8 region of the Ni-Ge phase diagram to display no additional ordering or superstructure.

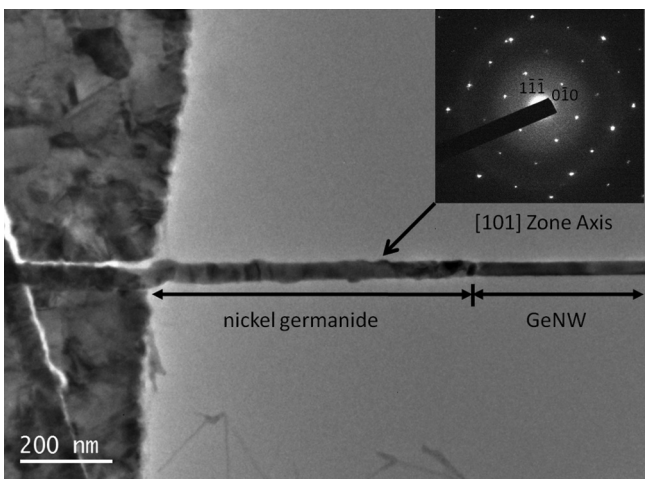

FIG. 2. TEM image of a Ni contact pad on a GeNW annealed at 400 °C for 2 min showing formation of an axial nickel germanide segment. The inset is a SAED pattern taken from the nickel germanide segment and is indexed as the Ni_2In prototype structure.

Annealing the Ni/GeNW samples at 400 °C for 2 min further increases the length of the nickel germanide segment to 660 nm on average. The nickel germanide segment is again found to be polycrystalline, and SAED patterns from each of the grains are matched to the prototype Ni_2In structure. Annealing of the samples at temperatures in excess of 450 °C results in fracture of the nickel germanide segment near the nickel germanide/GeNW interface, as shown in Fig. 3(a). A high magnification view of the break formed in the nickel germanide segment is shown in Fig. 3(b). Annealing samples at 500 or 600 °C for 2 min also results in a break near the nickel germanide/GeNW interface, and the nickel germanide segments are similar in length to those observed after annealing at 450 °C for 2 min. Therefore, regardless of whether samples are annealed at 450, 500, or 600 °C for 2 min, the break forms shortly after the axial nickel germanide segment is formed. The Ni supply is then cut off, resulting in similar nickel germanide segment lengths for all three annealing temperatures.

There are a number of possible explanations for why the nickel germanide nanowire segments break after annealing at or above 450 °C, some more plausible than others. One explanation involves unequal fluxes of Ni and Ge. To date, only one study by Marshall *et al.*[20] has been performed to identify the diffusing species in the formation of Ni germanides, specifically finding that Ni is the dominant diffusing species in the formation of Ni_2Ge. For the particular Ni germanide formed here, Ni_3Ge_2, the dominant diffusing species is not known. Perhaps Ge becomes the dominant diffusing species in Ni_3Ge_2 at or above 450 °C, eventually leading to the formation of a void in the growing Ni germanide segment near the Ge NW. However, the break is always about 50 nm away

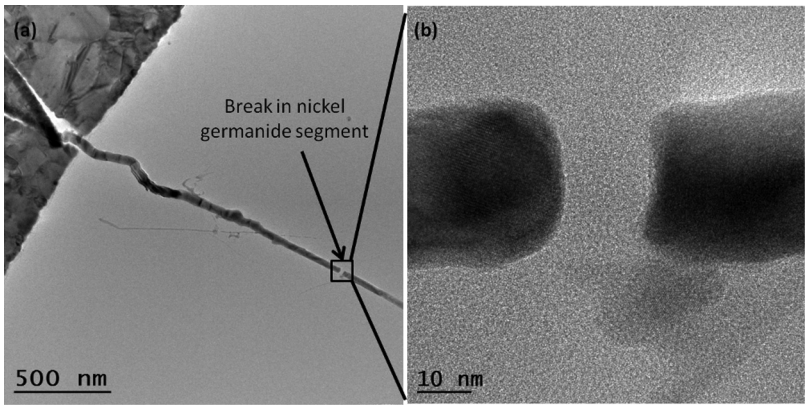

FIG. 3. (a) TEM image of a nickel germanide segment formed after annealing at 450 °C for 2 min showing the break that forms in the nickel germanide segment. (b) Higher magnification image of the broken nickel germanide segment showing the rounded surfaces that form after the nanowire breaks.

from the Ge NW rather than right at the germanide/Ge NW interface, which leads to some doubt about this explanation. A less likely explanation is that the germanides segment begins to agglomerate, akin to the agglomeration of NiGe thin films on Ge wafers at temperatures as low as 500° (Ref. 21) or the Rayleigh instability observed in other nanowires.[22,23] However, the germanides nanowire segment in our study does not break into beads anywhere else along its length, making this explanation less likely. Another possible explanation involves stress in the nanowire created by the thermal expansion mismatch between the nickel germanide segment and the GeNW. During rapid heating and cooling cycles in the RTA, perhaps a crack initially forms in the nanowire to relieve stress. It is also conceivable that more than one of these factors is at play.

The break in the wires at annealing temperatures of 450 °C and higher does not eliminate the possibility of forming longer nickel germanide segments. In order to form longer nickel germanide segments without breaking the NWs, lower annealing temperatures may be used for longer times. For example, annealing at 400 °C for 5 min results in forming nickel germanide segments with average lengths of 1.5 μm. Under these annealing conditions, axial nickel germanide contacts can be incorporated into structures such as those described by Sarpatwari *et al.*[24] in order to study the Schottky barrier height of axial contacts to semiconductor NWs or to reduce the access resistance of GeNW transistors.

In summary, we have found that Ni contact pads react with GeNWs to form axial nickel germanide segments after annealing at 350 °C for 2 min. Fracture in the nickel germanide segment occurs near the nickel germanide/GeNW interface for annealing temperatures of 450 °C or higher, but long segments may be grown if the annealing temperature is limited to 400 °C and longer annealing times are used. The ability to grow long nickel germanide segments microns in length will be useful for incorporation of nickel germanide contacts into GeNW field effect transistors and other nanoelectronic devices.

The authors are grateful for financial support from NSF through Grant No. ECS-0609282 and the Penn State Center for Nanoscale Science (Grant No. DMR-0820404) as well as the use of the Penn State Nanofabrication Facility (Grant No. NSF NNUN ECCS-0335765).

[1]D. Wang, Q. Wang, A. Javey, R. Tu, H. Dai, H. Kim, P. C. McIntyre, T. Krishnamohan, and K. C. Saraswat, Appl. Phys. Lett. **83**, 2432 (2003).
[2]M. Koto, P. W. Leu, and P. C. McIntyre, J. Electrochem. Soc. **156**, K11 (2009).
[3]S. M. Sze and K. K. Ng, *Physics of Semiconductor Devices* (Wiley, New York, 2007), p. 789.
[4]Y. Maeda, N. Tsukamoto, Y. Yazawa, Y. Kanemitsu, and Y. Masumoto, Appl. Phys. Lett. **59**, 3168 (1991).
[5]C. Lavoie, F. M. d'Heurle, C. Detavernier, and C. Cabral, Jr., Microelectron. Eng. **70**, 144 (2003).
[6]A. Dimoulas, A. Toriumi, and S. E. Mohney, MRS Bull. **34**, 522 (2009).
[7]M. Wittmer, M.-A. Nicolet, and J. W. Mayer, Thin Solid Films **42**, 51 (1977).
[8]Y. F. Hsieh, L. J. Chen, E. D. Marshall, and S. S. Lau, Thin Solid Films **162**, 287 (1988).
[9]F. Nemouchi, D. Mangelinck, C. Bergman, G. Clugnet, P. Gas, and J. L. Labar, Appl. Phys. Lett. **89**, 131920 (2006).
[10]L. J. Lin, K. L. Pey, W. K. Choi, E. A. Fitzgerald, D. A. Antoniadis, A. J. Pitera, M. L. Lee, D. Z. Chi, and C. H. Tung, Thin Solid Films **462–463**, 151 (2004).
[11]C. Perrin, D. Mangelinck, F. Nemouchi, J. Labar, C. Lavoie, C. Bergman, and P. Gas, Mater. Sci. Eng., B **154–155**, 163 (2008).
[12]Y. F. Hsieh, L. J. Chen, E. D. Marshall, and S. S. Lau, Mater. Res. Soc. Symp. Proc. **91**, 467 (1987).
[13]W.M. Weber, L. Geelhaar, E. Unger, C. Cheze, F. Kreupl, H. Riechert, and P. Lugli, Phys. Status Solidi B **244**, 4170 (2007).
[14]Y. Wu, J. Xiang, C. Yang, W. Lu, and C. M. Lieber, Nature (London) **430**, 61 (2004).
[15]N. S. Dellas, B. Z. Liu, S. M. Eichfeld, C. M. Eichfeld, T. S. Mayer, and S. E. Mohney, J. Appl. Phys. **105**, 094309 (2009).
[16]T. Burchhart, A. Lugstein, Y. J. Hyun, G. Hochleitner, and E. Bertagnolli, Nano Lett. **9**, 3739 (2009).
[17]P. Villars, L. D. Calvert, and W. B. Pearson, *Pearson's Handbook of Crystallographic Data for Intermetallic Phases*, 2nd ed. (American Society for Metals, Metals Park, OH, 1991), pp. 3739–3743.
[18]M. Ellner, T. Godecke, and K. Schubert, J. Less-Common Met. **24**, 23 (1971).
[19]A-K. Larsson and R. Withers, J. Alloys Compd. **264**, 125 (1998).
[20]E. D. Marshall, C. S. Wu, C. S. Pai, D. M. Scott, and S. S. Lau, Mater. Res. Soc. Symp. Proc. **47**, 161 (1985).
[21]Q. Zhang, N. Wu, T. Osipowicz, L. K. Bera, and C. Zhu, Jpn. J. Appl. Phys. **44**, L1389 (2005).
[22]W. Hu, B. Liu, N. S. Dellas, S. M. Eichfeld, S. E. Mohney, J. M. Redwing, and T. S. Mayer, Proc. SPIE **7610**, 76100V (2010).
[23]F. A. Nichols and W. W. Mullins, J. Appl. Phys. **36**, 1826 (1965).
[24]K. Sarpatwari, N. S. Dellas, O. O. Awadelkarim, and S. E. Mohney, Solid-State Electron. **54**, 689 (2010).